



## OPEN ACCESS

EDITED BY  
Gaurisankar Sa,  
Bose Institute, India

REVIEWED BY  
Arindam Maitra,  
National Institute of Biomedical  
Genomics (NIBMG), India  
Gunes Esendagli,  
Hacettepe University, Turkey

\*CORRESPONDENCE  
Kejin Wu  
kejinwu@163.com

†These authors have contributed  
equally to this work and share  
first authorship

SPECIALTY SECTION  
This article was submitted to  
Cancer Immunity  
and Immunotherapy,  
a section of the journal  
Frontiers in Immunology

RECEIVED 24 April 2022  
ACCEPTED 29 July 2022  
PUBLISHED 18 August 2022

CITATION  
Geng S, Fu Y, Fu S and Wu K (2022)  
A tumor microenvironment-related  
risk model for predicting the  
prognosis and tumor immunity  
of breast cancer patients.  
*Front. Immunol.* 13:927565.  
doi: 10.3389/fimmu.2022.927565

COPYRIGHT  
© 2022 Geng, Fu, Fu and Wu. This is an  
open-access article distributed under  
the terms of the [Creative Commons  
Attribution License \(CC BY\)](https://creativecommons.org/licenses/by/4.0/). The use,  
distribution or reproduction in other  
forums is permitted, provided the  
original author(s) and the copyright  
owner(s) are credited and that the  
original publication in this journal is  
cited, in accordance with accepted  
academic practice. No use,  
distribution or reproduction is  
permitted which does not comply with  
these terms.

# A tumor microenvironment-related risk model for predicting the prognosis and tumor immunity of breast cancer patients

Shengkai Geng<sup>†</sup>, Yipeng Fu<sup>†</sup>, Shaomei Fu and Kejin Wu\*

The Obstetrics and Gynecology Hospital of Fudan University, Shanghai, China

**Background:** This study aimed to construct a tumor microenvironment (TME)-related risk model to predict the overall survival (OS) of patients with breast cancer.

**Methods:** Gene expression data from The Cancer Genome Atlas was used as the training set. Differentially expressed gene analysis, prognosis analysis, weighted gene co-expression network analysis, Least Absolute Shrinkage and Selection Operator regression analysis, and Wald stepwise Cox regression were performed to screen for the TME-related risk model. Three Gene Expression Omnibus databases were used to validate the predictive efficiency of the prognostic model. The TME-risk-related biological function was investigated using the gene set enrichment analysis (GSEA) method. Tumor immune and mutation signatures were analyzed between low- and high-TME-risk groups. The patients' response to chemotherapy and immunotherapy were evaluated by the tumor immune dysfunction and exclusion (TIDE) score and immunophenscore (IPS).

**Results:** Five TME-related genes were screened for constructing a prognostic signature. Higher TME risk scores were significantly associated with worse clinical outcomes in the training set and the validation set. Correlation and stratification analyses also confirmed the predictive efficiency of the TME risk model in different subtypes and stages of breast cancer. Furthermore, immune checkpoint expression and immune cell infiltration were found to be upregulated in the low-TME-risk group. Biological processes related to immune response functions were proved to be enriched in the low-TME-risk group through GSEA analysis. Tumor mutation analysis and TIDE and IPS analyses showed that the high-TME-risk group had more tumor mutation burden and responded better to immunotherapy.

**Conclusion:** The novel and robust TME-related risk model had a strong implication for breast cancer patients in OS, immune response, and therapeutic efficiency.

## KEYWORDS

breast cancer, tumor microenvironment, prognostic factor, tumor immunity, therapeutic efficiency

## Introduction

In recent years, breast cancer has become the most frequently diagnosed cancer for women globally (1–3). In China, breast cancer, with the highest incidence, is the leading cause of cancer-related mortality in females (4, 5). With increasing importance attached to individualized precision therapy, the traditional tumor–node–metastasis (TNM) stage system and molecular typing PAM50 had been challenged since the prognosis or treatment response of patients at the same stage or with the same molecular subtype could vary substantially due to the heterogeneity of the tumor (6). Thus, the average treatment benefits for unselected patients are low, motivating tumor biology-based selection strategies *via* gene expression assays (GEAs) including Oncotype DX (7), MammaPrint in luminal early breast cancer (8–11), and Fudan University Shanghai Cancer Center gene panel in metastatic triple-negative breast cancer (TNBC) (12). However, the strategies mentioned above were strictly refined to certain molecular subtypes; this called for a universal method to stratify breast cancer patients across different molecular subtypes.

The tumor microenvironment (TME) plays an essential role in the occurrence and development of cancer (13–15), which is reflected by the various immune cells, stromal cells, cytokines, and extracellular matrix molecules existing in the microenvironment. Accumulating evidence had demonstrated that immune cells, as components of TME, were significantly associated with a breast cancer patient's therapy efficiency and prognosis (16, 17). In addition, research (18–20) revealed that stromal cells recruited by cancer cells from nearby endogenous host stroma were significantly associated with events such as tumor angiogenesis, proliferation, invasion, and metastasis. Furthermore, the extensive cross-talk between immune and stromal cells had a profound influence on a breast cancer patient's prognosis (21). To date, TME was increasingly considered as a target for combination therapy in patients with breast cancer (21). Previous studies (22–27) had focused on the involvement of TME in the combination with conventional therapies to boost therapeutic responses and prolong the survival of breast cancer patients. However, few studies reported that TME could also be used as a prognostic factor for breast cancer patients, let alone the significance of TME in predicting tumor immunity and therapeutic efficiency for breast cancer patients. Therefore, with proper evaluation, it is

reasonable to dig further into the predictive factor of TME in breast cancer patients.

In 2013, Yoshihara *et al.* constructed a new algorithm called ESTIMATE algorithm (28) to infer the proportion of stromal and immune cells in tumor samples. Previous studies had proved the ESTIMATE algorithm to be an effective tool in predicting the TME status (29). In this study, we used ESTIMATE algorithm (28) to calculate the immune, stromal, and ESTIMATE scores and to evaluate the TME status in breast cancer. Gene expression data from The Cancer Genome Atlas (TCGA) were used to establish a TME risk prognostic model based on TME-related genes. Gene Expression Omnibus (GEO) databases were used to validate the predictive efficiency of the prognostic model. Gene set enrichment analysis (GSEA) method was used to explore the possible immune function involved in the TME risk model. Furthermore, the correlation between the TME risk model and tumor mutation burden as well as immunotherapy efficiency was also investigated.

## Materials and methods

### Data collection

The RNA-normalized sequencing data (1,053 breast cancer tissues and 111 matched normal tissues, fragment per kilobase per million) and corresponding clinical information (including clinical characteristics and tumor mutation status) of patients with breast cancer were downloaded from the TCGA database (19 patients without corresponding clinical information were excluded). Normalized gene expression data of GSE158309, GSE17705, and GSE31448 were downloaded from the GEO database. Genome-wide co-expression analysis was performed to investigate potential TME- and prognosis-related genes based on the TCGA database. The datasets from GEO database were independently used for external validation. Immune score, stromal score, and tumor purity were calculated using the ESTIMATE algorithm (28) provided in the R package “estimate”.

### Development of the TME-related prognostic gene signature

Differentially expressed gene (DEG) analysis was performed using the edgeR filtering method included in the “Limma” R

package. TME-related DEGs were defined as genes whose false discovery rate (FDR) value was  $<0.05$  and  $\log_2$  (fold change) was  $>1$ . Weighted gene co-expression network analysis (WGCNA) was performed to recognize gene modules related to the immune and stromal scores. Gene modules with a correlation coefficient  $>0.5$  were considered as strong TME-correlated modules. Univariate Cox regression analysis was used to recognize prognostic genes ( $p < 0.05$ , two-tailed) for patients with breast cancer in the TCGA dataset. The intersections of the immune- and stromal-related genes screened by DEGs, WGCNA, and univariate Cox regression analyses were all inputted in the Least Absolute Shrinkage and Selection Operator (LASSO) regression analysis to identify the hub genes. The combination of two hub genes was inputted into the Wald stepwise Cox regression to develop the TME risk model. In this process, the model with minimal Akaike information criterion (AIC) value was determined as the final mode. The signature was defined as TME risk score =  $\sum \text{coefficient-mRNA}_i \times \text{expression of mRNA}_i$ . Receiver operating characteristic curve (ROC) analysis was used to determine the optimal cutoff value for the high- and low-TME-risk groups in SPSS version 25 (SPSS Inc.).

## Survival and immune analysis for low- and high-TME-risk groups

ROC analysis was used to determine the optimal cutoff value of the TME risk score for patients' overall survival (OS). After the patients from the TCGA dataset were divided by the cutoff value of the TME risk score, we used t-distributed stochastic neighbor embedding (t-SNE) and principal component analysis (PCA) to evaluate the discrimination of the model. The association of clinicopathologic characteristics and stromal-immune scores between low- and high-TME-risk groups was analyzed using a two-sided chi-square test. The survival curves were determined by the Kaplan–Meier analysis and compared by the log-rank test. The Cox proportional hazards regression model was used to perform univariate and multivariate analyses, and  $P < 0.05$  (two-tailed) was considered statistically significant. We used the time-dependent area under the receiver operating characteristic curve (AUC) and C statistics to evaluate the predictive power of TME risk for OS. Calibration plots were used to evaluate the discriminative ability and accuracy of the models. Stage- and subtype-stratified analyses of prognostic significance of TME risk in patients with breast cancer were performed. The HUMAN PROTEIN ATLAS (HPA) database and Gene Expression Profiling Interactive Analysis (GEPIA) were used to evaluate the immunohistochemical (IHC) staining and the prognostic significance of the TME risk signature. The expression of the human leukocyte antigen (HLA) gene family and immune checkpoints (30, 31) was evaluated in both low- and high-TME-risk groups. The population abundance of tissue-infiltrating immune and stromal immune and stromal cells were

calculated with different methods, including TIMER (32), CIBERSORT (33), and Xcell (34) algorithms (available at TIMER2.0 website, <http://timer.comp-genomics.org/>). The correlation between the hub genes and different immune cell infiltration was evaluated using the Wilcoxon test.

## Function enrichment and tumor mutation status analysis in the low- and high-TME-risk groups

The biological function related to TME risk was investigated using the GSEA method. FDR  $q$ -value  $<0.05$  and  $|\text{normalized enriched score (NES)}| >1$  were considered significantly enriched. Then, we evaluated the function enrichment of the identified TME risk genes using Gene Ontology (GO) function analysis (including biological process, cellular component, and molecular function) and Kyoto Encyclopedia of Genes and Genomes (KEGG) analysis. After downloading the breast cancer patient's tumor mutation information from the TCGA database, different mutation types were evaluated in both the high- and low-TME-risk groups. In addition, tumor mutational burden (TMB) and mutation counts were calculated to find the potential correlation between TME risk and tumor mutation status. Stratified analysis was performed to investigate the tumor mutation difference in different subtypes. The Spearman method was used to calculate the correlation coefficient, and  $P < 0.05$  (two-tailed) was considered statistically significant.

## Prediction of immune escape and immunotherapy efficiency in patients in groups with different TME risks

We used the pRRophetic algorithm in R language to evaluate the 50% inhibiting concentration (IC50) value of the 88 drugs in the low- and high-TME-risk groups. The potential response of patients to immunotherapy was inferred by the immunophenscore (IPS) (35) (downloaded from The Cancer Immune Group Atlas, TCIA) and tumor immune dysfunction and exclusion (TIDE) score.

## Results

### Correlation of the clinical features of patients with breast cancer with immune/stromal scores

A total of 1,164 samples (111 normal tissue samples and 1,053 breast cancer samples) in the TCGA database were included in our study to calculate the immune and stromal scores. The stromal scores of these patients ranged from -2,033.4

to 2,083.4, and the immune scores ranged from -1,162.0 to 3,638.8. There were no significant differences between normal and breast cancer tissues in relation to immune scores, while normal tissue had higher stromal scores than breast cancer samples. The correlation of the clinicopathological characteristics in breast cancer patients between different groups is presented in [Supplementary Figure S1](#). In our study, the immune and stromal scores had no significantly different distribution in the old/young patients, T stage, N stage, and TNM stage. In addition, the survival analysis showed that patients with higher immune scores had a more favorable OS than those with lower immune scores.

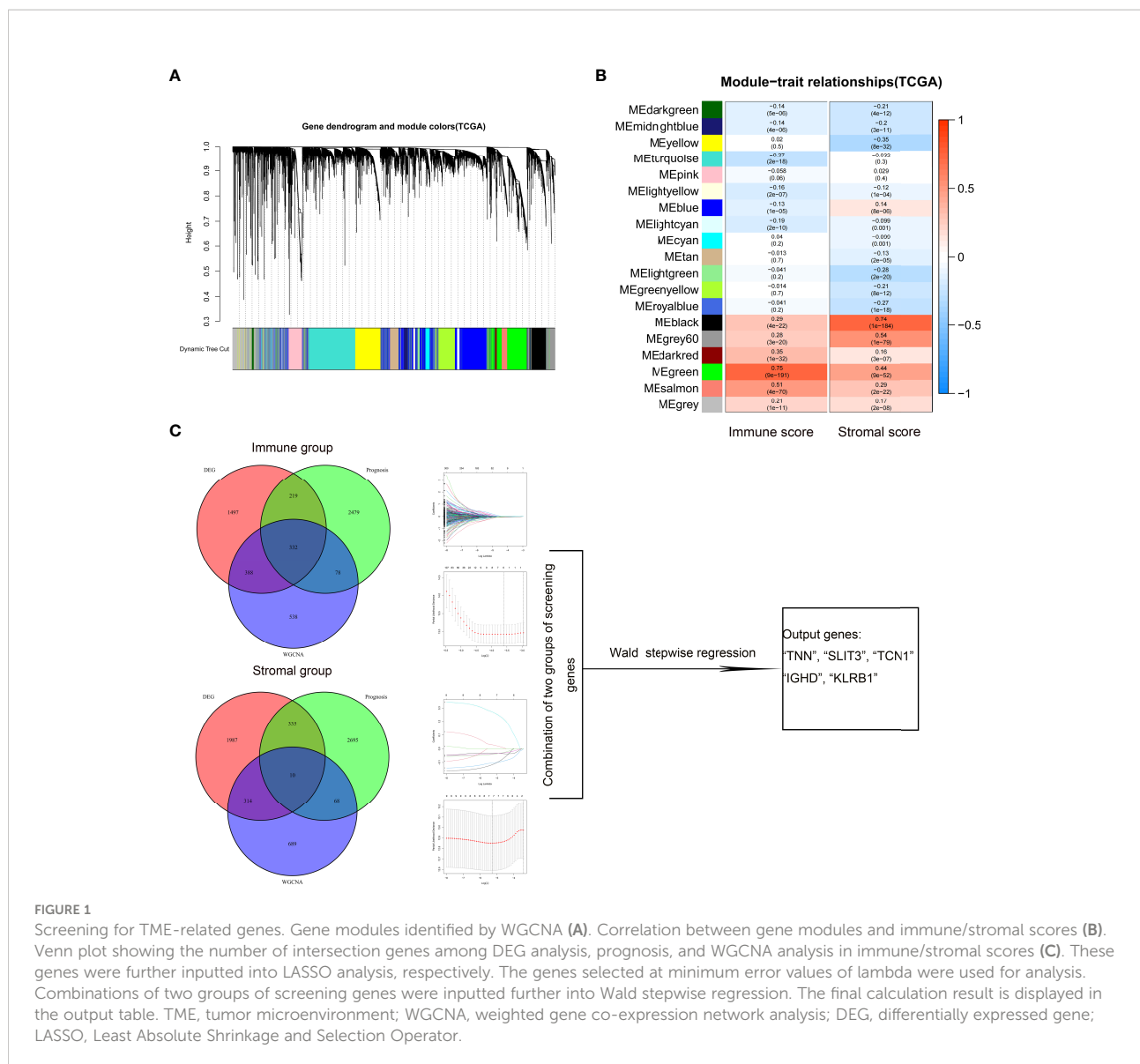
## Development of a prognostic TME risk signature with the TCGA cohort

Divided by the median value of immune/stromal scores, the DEG analysis between the low- and high-immune/stromal score groups was performed using the edgeR filtering method. In our study, six was selected as the optimal soft threshold of WGCNA. As shown in [Figure 1](#), 19 co-expressed gene modules were recognized in relation to immune/stromal scores. The green and salmon had a strong correlation with the immune score, whereas the gray and black were associated with the stromal score. Univariate Cox regression analysis was used to recognize the prognostic genes for the groups with different immune/stromal scores. The Venn plot showed the intersection of DEGs, TME-risk-correlated gene modules, and prognostic genes. After the LASSO-Cox regression analysis, IGHA1, PIGR, APOBEC3D, IGHD, KLRB1, and MATK were selected from the immune score group, whereas MEOX1, COL12A1, HSD11B1-AS1, TNN, SLIT3, TCN1, and CPXM1 were selected from stromal score group. A combination of two groups of screening genes was further inputted into Wald stepwise regression analysis to develop the final model (the result is presented in [Supplementary Table S1](#)). With the minimal AIC (AIC = 1,546.21), the final model was as follows: TME risk = SLIT3 \* 0.329 - TNN \* 0.11 - TCN1 \* 0.051 - IGHD \* 0.075 - KLRB1 \* 0.164.

## Correlation and stratification analyses of TME risk and validation of the prognostic model

In our study, patients from TCGA were divided into low- and high-TME-risk groups by the optimal cutoff value of TME risk score (1.167) for breast cancer patient's OS. The PCA and t-SNE analyses demonstrated that patients with different TME risk scores were well separated in two directions (shown in [Supplementary Figures S2A, B](#)). The correlation between the patients' clinicopathological characteristics and TME risk scores

is shown in [Figure 2](#). In our study, we found that higher TME risk scores were associated with higher age, higher T stage, and higher TNM stage. The Kaplan-Meier (KM) analysis showed that the low-TME-risk group of patients with breast cancer had a more favorable clinical outcome ( $P < 0.001$ ). The AUC (for predicting the patients' OS of 1, 3, and 5 years, this was 0.696, 0.708, and 0.689, respectively) and the calibration plot analyses both confirmed the predictive ability of TME risk score (shown in [Figure 3A](#)). The survival analysis showed a significantly negative correlation between the TME risk score and patients' OS. The ROC analysis showed that the C statistics of TME risk was 0.64 (95%CI: 0.592–0.688,  $P = 0.024$ ). Furthermore, the stage-stratified analysis showed that the TME risk score was identified as a prognostic factor for all breast cancer stages ( $P = 0.037$  for stage I patients,  $P < 0.001$  for stage II patients, and  $P < 0.001$  for stage III patients; shown in [Supplementary Figures S3A–C](#)). In addition, the subtype-stratified analysis showed that HR-positive and TNBC patients with lower TME risk scores had a more favorable OS ( $P < 0.001$  and  $P = 0.008$ , respectively; shown in [Supplementary Figures S3D–F](#)). The validation was performed on three GEO datasets (GSE 31448, GSE158309, and GSE17705). The KM analysis in all datasets confirmed the significant association between TME risk and patients' OS. As shown in [Figure 3B](#), the GSE31448 dataset proved the TME risk score prognostic ability in all subtypes of breast cancer patients. The AUC for predicting the patients' OS of 1, 3, and 5 years was 0.689, 0.643, and 0.677, respectively. To evaluate the long-term outcome prediction of TME risk score, GSE17705 (ER-positive subtype breast cancer patients) and GSE158309 (early breast cancer patients) datasets were enrolled in our study. Both datasets confirmed the association between the TME risk score and the patients' OS. The AUC for predicting the patients' OS of 10, 12, and 15 years was 0.580, 0.675, and 0.652 in ER-positive breast cancer patients and that of 8, 10, and 12 years was 0.655, 0.619, and 0.634 in early breast cancer patients, respectively. Similarly, good concordance was observed between the model predicted and the actual observations in three calibration curves. The C statistics of the three datasets are presented in [Figure 3](#), showing that TME risk score had a good predictive effect (GSE31448—0.639, 95%CI: 0.565–0.713,  $P = 0.038$ ; GSE17705—0.597, 95%CI: 0.51–0.663,  $P = 0.039$ ; GSE158309—0.609, 95%CI: 0.513–0.706,  $P = 0.049$ ). Furthermore, we used HPA database and GEPIA to evaluate the IHC staining and the prognostic significance of the TME risk signature. The KM analysis, along with the typical IHC staining of SLIT3, TNN, IGHD, and KLRB1, showed that the expression was significantly different between normal and breast cancer tissues and confirmed the prognostic effect of the TME risk signature. The UMAP results of single-cell sequencing (shown in [Supplementary Figure S5](#)) showed that SLIT3 and TNN were mainly expressed in stromal cells, while IGHD and KLRB1 were mainly enriched in immune cells. In addition, TCN1 was found to be expressed mainly in breast glandular cells. Taken together,



our TME risk model integrated the stromal-immune signature, further confirming that breast cancer prognosis was significantly associated with the tumor microenvironment.

## Analysis of immune and functional enrichment studies between the low- and high-TME-risk groups

A total of 24 HLA-related genes and 39 immune checkpoints between the low- and high-TME-risk groups were investigated in our study. As shown in **Figures 2C, D**, all HLA family genes and 34 immune checkpoints were significantly different between the low- and high-TME-risk groups as evaluated by the Wilcoxon test. Compared with the high-TME-risk group, most

of the immune-related genes in the low-TME-risk group were upregulated, except the TNFSF4 and NRP1 immune checkpoints. To further explore the possible mechanisms underlying the differential expression of immune-associated genes between the low- and high-TME-risk groups, we performed the GSEA analysis with annotations based on the GO and KEGG gene databases. In total, 50 of the most significant enrichment results ( $|NES| > 1$  and FDR value  $< 0.05$ ) are presented in **Supplementary Figure S4**. We found that many biological processes related to immune response functions, including proliferation, migration, and infiltration of immune cells, inflammatory responses, chemokine activities, cellular defense responses, and leukocyte migration, were significantly associated with the low-TME-risk group. In addition, a clear inverse correlation was found between the TME risk score and

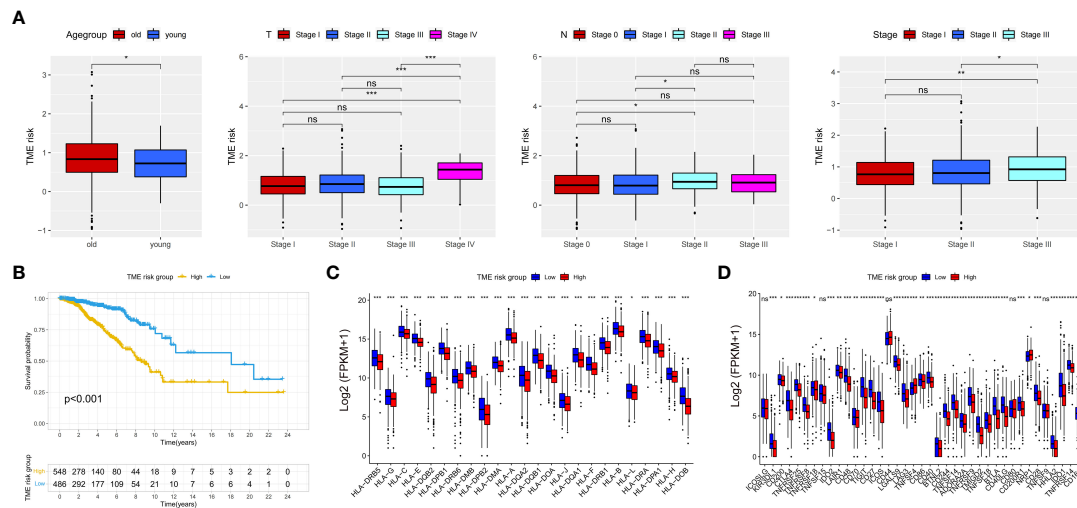


**FIGURE 2** Difference analysis of TME risk scores in age (age over 40 years old was defined as the old group, and age up to 40 years was defined as the young group), T stage, N stage, and TNM stage (A). Kaplan–Meier analysis between low- and high-TME-risk groups (B) (the low- and high-TME-risk groups were divided by the optimal cutoff value). Difference analysis for the expression of HLA family (C) and immunecheckpoint genes (D) between low- and high-TME-risk groups. TME, tumor microenvironment. The statistical difference was compared by pairwise comparisons using Wilcoxon test. Significance: \* $P < 0.05$ ; \*\* $P < 0.01$ ; \*\*\* $P < 0.001$ . ns, not significant.

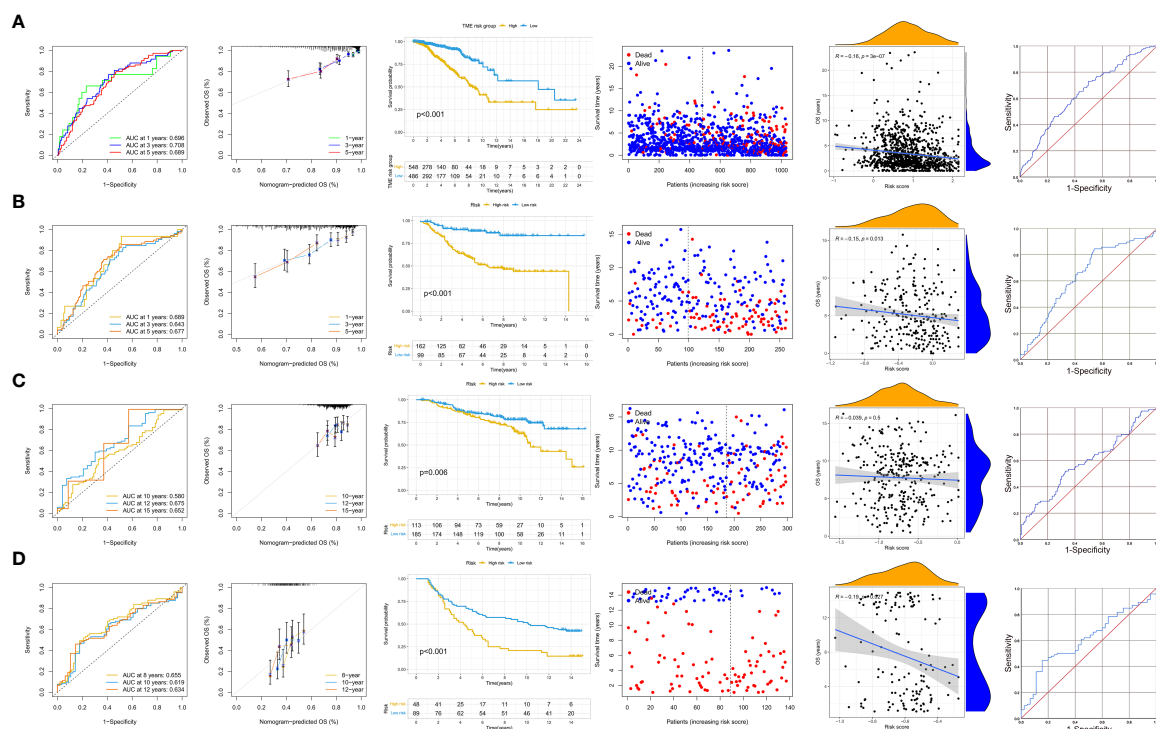


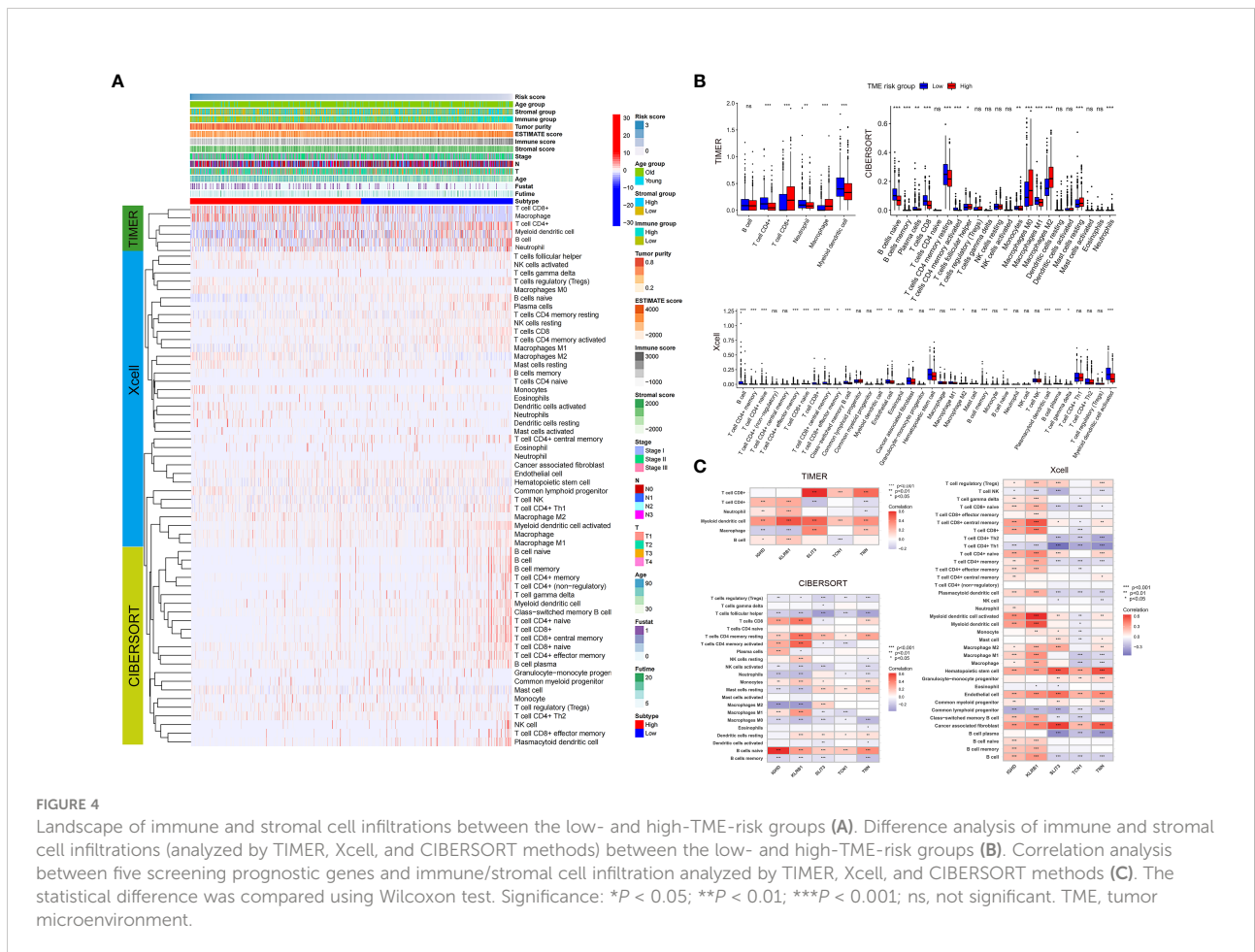
**FIGURE 3** AUC analysis, calibration analysis, Kaplan–Meier analysis, correlation between TME risk scores, and patients' OS and ROC analysis in the training set (A), validation set [GSE31448, all subtypes of breast cancer patients (B)], HR-positive breast cancer patients [GSE17705 (C)], and early-stage breast cancer patients [GSE158309 (D)]. AUC, area under the curve; TME, tumor microenvironment; OS, overall survival; ROC, receiver operating characteristic curve; HR, hormone receptor; Her-2, human epidermal growth factor receptor 2.

the immune/stromal score (shown in **Supplementary Figures S5A, B**), while the tumor purity score was in accordance with the TME risk tendency (shown in **Supplementary Figure S5C**). The hub genes' expression had a significantly distinct distribution between the low- and high-TME-risk groups (shown in **Supplementary Figures S5D-H**).

We then investigated the distribution of infiltrating immune cells as inferred by TIMER, CIBERSORT, and xCell between the low- and high-TME-risk groups (shown in **Figure 4**). Our study revealed that most of the immune and stromal cells, including B cells, T cells CD4+, T cells CD8+, and myeloid dendritic cells, increased in the low-TME-risk group. However, macrophages (especially macrophage II) infiltrated more in the high-TME-risk group, while there was no uniform result in terms of neutrophils. Meanwhile, we did not find significant differences in T cells CD4+ Th1/Th2 and NK cells between the two groups.

## The correlation between TME risk and tumor mutation status

We downloaded the breast cancer patient's tumor mutation information from the TCGA database to evaluate its correlation with the TME risk score. As shown in **Figure 5**, more somatic mutations were presented in the high-TME-risk group, while the maftools analysis results showed no significant differences between the low- and high-TME-risk groups in terms of the mutation frequencies of specific genes. Furthermore, the KM analysis revealed that the combination of TMB and TME risk had profound effects on patients' prognosis, and patients with high TME risk and high TMB tended to have the worst clinical outcome. What is more, the subtype-stratified analysis showed a clear positive association between TME risk score and TMB in ER-positive and TNBC breast cancer patients, which might partly reflect the connection with patients' prognosis.



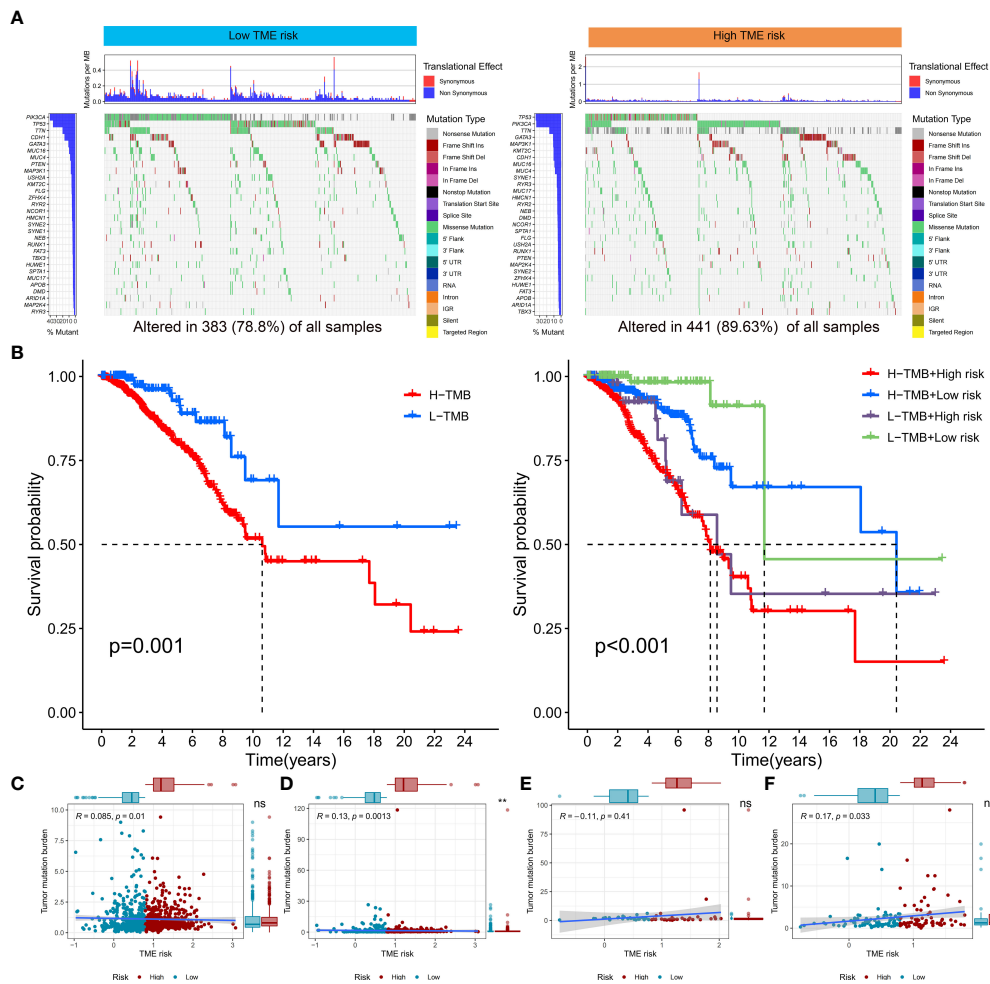


**FIGURE 5** Landscape of TMB and tumor mutation status in low- and high-TME-risk groups (A). Kaplan–Meier analysis between low- and high-TME-risk groups combined with low- and high-TMB groups (B). Association between breast cancer patient's TMB (C) all patients, (D) HR-positive breast cancer patients, (E) Her-2 positive breast cancer patients, and (F) TNBC patients) and distribution in groups with different TME risks. TMB, tumor mutation burden; TME, tumor microenvironment; HR, hormone receptor; Her-2, human epidermal growth factor receptor 2; TNBC, triplenegative breast cancer. The statistical difference was compared by pairwise comparisons using Wilcoxon test. Significance: \* $P < 0.05$ ; \*\* $P < 0.01$ ; \*\*\* $P < 0.001$ . ns, not significant.

## Immune escape and immunotherapy efficiency between low- and high-TME-risk groups

In our study, we used the IC50 value of the 88 drugs to evaluate the TME risk score as a predictive factor for the response of breast cancer patients to therapies (including chemotherapy, targeted therapy, and immunotherapy). Several commonly used clinical drugs are presented in Figure 6. We found that patients with a higher TME risk score had lower TIDE scores and higher IPS scores. These results suggested that patients in the high-TME-risk group were more likely to respond better to immunotherapy. In accordance with the TIDE score, immune dysfunction and exclusion analysis also showed that

patients with higher TME risk scores might benefit more from immunotherapy. In addition, the IC50 analysis showed that patients in the high-TME-risk group might be more sensitive to imatinib and lapatinib, while patients in the low-TME-risk group might be more sensitive to palbociclib, paclitaxel, cisplatin, veliparib, etc.

## Discussion

In our study, we constructed a novel, easy-to-use, and effective TME risk score system based on immune and stromal scores for the prediction of breast cancer patient's OS. First, our results showed that the TME risk was an independent prognostic

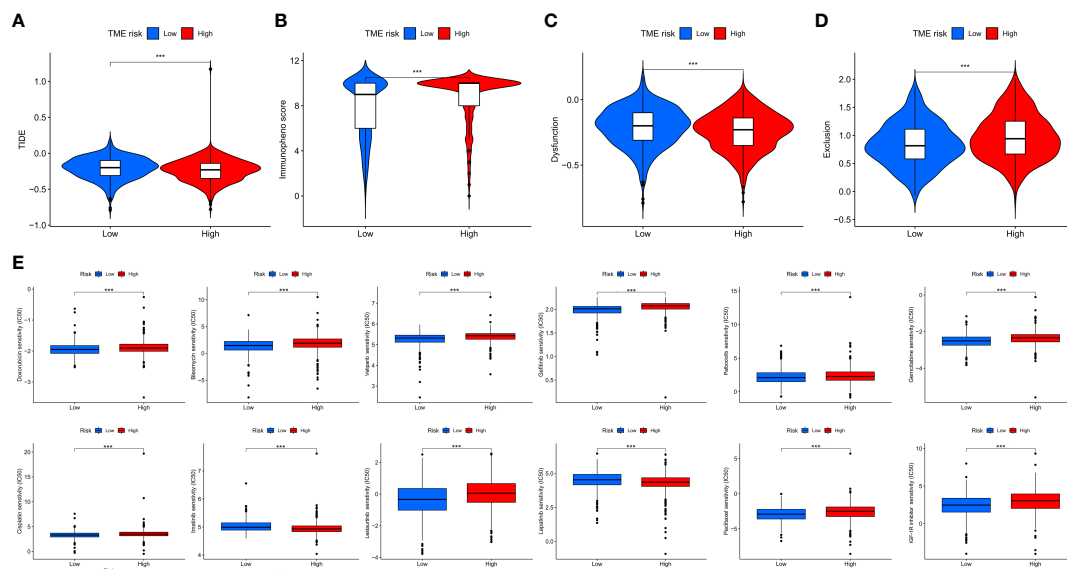


FIGURE 6

TIDE analysis (A), IPS analysis (B), immune dysfunction analysis (C), and immune exclusion analysis (D) between low- and high-TME-risk group. Difference analysis (E) of commonly used clinical drugs' chemotherapeutic responses including doxorubicin, bleomycin, veliparib, gefitinib, palbociclib, gemcitabine, cisplatin, imatinib, testauntinib, lapatinib, paclitaxel, and IGF-1R inhibitor between low- and high-TME-risk groups. Statistical difference was compared using Wilcoxon test. Significance: \* $P < 0.05$ ; \*\* $P < 0.01$ ; \*\*\* $P < 0.001$ . ns, not significant; TIDE, tumor immune dysfunction and exclusion; IPS, immunophenoscore; TME, tumor microenvironment.

factor for all breast cancer patients. With the stratified analysis and external validation of GEO datasets, we confirmed the predictive efficiency of TME risk in all stages of breast cancer patients, especially in early stage, TNBC, and HR-positive breast cancer patients. In addition, our study showed that patients in the low-TME-risk group presented higher levels of immune and stromal cell infiltration, higher immunogenicity, lower tumor purity, and lower somatic mutation status than patients in the high-TME-risk group. Furthermore, a positive association was found between TME risk and TMB status, the combination of which might have a significant prognostic value for breast cancer patients. Finally, the TIDE and IPS score analyses demonstrated that TME risk could be a potential biomarker for predicting immunotherapeutic response for breast cancer patients.

The TME risk score was constructed based on the immune and stromal scores calculated by the ESTIMATE algorithm. Previous studies had demonstrated the prognostic value of this algorithm in many diseases, such as gastric adenocarcinoma (36, 37), colon cancer (38), lung adenocarcinoma (39), clear cell renal cell carcinoma (40), *etc.* The effect of tumor-infiltrating lymphocytes on breast cancer patients' clinical outcomes was well established in previous research (41, 42). In accordance with the previous studies, we found that patients with better prognosis had higher immune scores, while no significant overall association of clinical characteristics of breast cancer with stromal score alone was observed. However, the TME risk score, calculated based on the combination of immune and

stromal scores, was identified to be significantly associated with breast cancer patients' T stage, TNM stage, and OS, indicating that we should not separately look at the impact of immune and stroma on the prognosis of breast cancer. In addition, the stratified analysis revealed that the TME risk was an independent prognostic factor for patients in different TNM stages. For HR-positive patients and TNBC, the high TME risk was significantly associated with worse clinical outcomes. Furthermore, the robust performance of the TME risk model for long-term prognosis in HR-positive and early breast cancer patients was confirmed by the AUC analyses in three independent GEO datasets. The calibration curves and correlation analysis also showed good concordance between the model predicted and the actual observations. Additionally, the analysis of drug sensitivity revealed that the TME risk model influenced the patients' drug response to chemotherapy and targeted therapy. The IC<sub>50</sub> analysis showed that patients in the high-TME-risk group might be more sensitive to imatinib and lapatinib, while patients in the low-TME-risk group might be more sensitive to palbociclib, paclitaxel, cisplatin, veliparib, *etc.* Taken together, our results revealed that the TME risk prognostic model might aid physicians in making clinical therapy decisions and guiding the long-term follow-up to let breast cancer patients gain survival benefits.

Maintaining a good predictive value, our final prognostic model included only five genes selected based on the stromal and immune scores, which could reduce the patients' unnecessary

waste. TNN, known as Tenascin-N or -W, was involved in neurite outgrowth and cell migration in hippocampal explants. In tumors, it stimulates angiogenesis by the elongation, migration, and sprouting of endothelial cells (43). In terms of breast cancer, it was significantly downregulated in tumor samples and might facilitate tumorigenesis by supporting the migratory behavior of breast cancer cells (44). SLIT3 was involved in the final model, and previous researches had demonstrated that the suppression of SLIT3 might induce tumor proliferation and invasion in many solid tumors such as ovarian cancer (45), hepatocellular carcinoma (46), thyroid cancer (47), and gastric cancer (48). TCN1 (Transcobalamin I, vitamin B12 binding protein, R binder family) encodes a member of the vitamin B12-binding protein family. This family of proteins, alternatively referred to as R binders, is expressed in various tissues and secretions. Previous research had shown that a high expression of TCN1 was a negative prognostic factor in colon cancer and might correlate with the patients' chemosensitivity (49–51). The TME risk prognostic model also included immune-related genes (KLRB1 and IGHD). Proteins coded by these genes were associated with the immune microenvironment (52) and immune cell infiltration (53) (such as natural killer cells and T cells). In our study, the low-TME-risk group upregulated in many immune checkpoints and increased in most of the immune and stromal cells, including B cells, T cells CD4+, T cells CD8+, and myeloid dendritic cells. In addition, the function analyses (GO and KEGG) revealed that many biological processes related to immune response functions were significantly associated with the low-TME-risk group. Taken together, these might be why patients in the low-TME-risk group had a better prognosis.

Immunotherapy, as an emerging novel treatment modality, is increasingly applied in the treatment of cancer patients (54–56). However, the optimal patient selection who may benefit from immunotherapy remains a great challenge. Recent studies had proved TMB as an emerging biomarker of response to immunotherapy for many cancers (57–59). As shown in Figure 5, more somatic mutations were presented in the high-TME-risk group. In addition, the stratified analysis showed a positive correlation between TME risk and TMB, especially in ER-positive and TNBC patients. What is more, the combination of TMB and TME risk had a profound implication for prognosis. Patients with higher TME risk scores and higher TMB tended to have the worse clinical outcome. Our study revealed that the high-TME-risk group might respond better to immunotherapy using TIDE and IPS score analysis, which was in accordance with the tumor mutation status and previous research. In addition, patients in the high-TME-risk group tended to have lower immune cell infiltration and downregulation of HLA and immune checkpoint expressions. It should be noted that the TNFSF4

and NRP1 immune checkpoints were upregulated in the high-TME-risk group. Previous studies had proved that VEGF-A/NRP1 signaling might be associated with breast cancer metastasis (60, 61). The study (62) by Kai Li *et al.* also revealed the oncogenic features of TNFSF4 and specifically demonstrated the potential effects of applying TNFSF4 blockade-based immunotherapies in breast carcinomas. Taken together, our results might suggest potential therapeutic targets and provide novel clinical applications for immunotherapies.

There were several limitations in our studies. Firstly, due to the lack of clinical details of breast cancer patients in public databases (such as menopause status and chemotherapy regimens), we cannot perform a more in-depth stratification analysis between the low- and high-TME-risk groups. Secondly, database information on immune infiltration and stroma status was inferred by TIMER, CIBERSORT, and xCell between the low- and high-TME-risk groups only using the expression data of immune-associated genes.

## Conclusion

In conclusion, our study successfully constructed and validated a novel and robust TME-related prognostic model for breast cancer patients. Furthermore, our predictive model could seek the possibility to find selected patients who would benefit more from anticancer immunotherapy and adjuvant chemotherapy, which would reduce the risk of complications and give the patients better individual treatment guidance.

## Data availability statement

The RNA-seq data and corresponding clinical information were observed from the TCGA (<https://portal.gdc.cancer.gov/>) and GEO (<https://www.ncbi.nlm.nih.gov/geo/>). The IPS for breast cancer patients were retrieved from the TCIA (<https://tcia.at/home>). The accession number(s) can be found in the article/Supplementary Material.

## Ethics statement

The studies involving human participants were reviewed and approved by TCGA and GEO databases. The patients/participants provided their written informed consent to participate in this study. Written informed consent was obtained from the individual(s) for the publication of any potentially identifiable images or data included in this article.

## Author contributions

All authors participated in the design, interpretation of the studies, analysis of the data, and review of the manuscript. SG and YF conceived and designed the whole project and wrote the manuscript. SG and YF performed the data analyses. SG, YF, and KW interpreted the data and partook in the discussion. SF and KW revised the final version of the manuscript. All authors contributed to the article and approved the submitted version.

## Funding

This work was supported by the National Natural Science Foundation of China (no. 81902993), Shanghai Health Committee (no. 2020YJZX0204), and Shanghai Shenkang Hospital Development Center (no. SHDC22020209).

## Acknowledgments

We would like to appreciate the TCGA, GEO, HPA, GEPIA, and TCIA database for the availability of the data.

## Conflict of interest

The authors declare that the research was conducted in the absence of any commercial or financial relationships that could be construed as a potential conflict of interest.

## Publisher's note

All claims expressed in this article are solely those of the authors and do not necessarily represent those of their affiliated organizations, or those of the publisher, the editors and the reviewers. Any product that may be evaluated in this article, or claim that may be made by its manufacturer, is not guaranteed or endorsed by the publisher.

## References

- DeSantis C, Ma J, Bryan L, Jemal A. Breast cancer statistics, 2013. *CA: Cancer J Clin* (2014) 64(1):52–62. doi: 10.3322/caac.21203
- DeSantis CE, Ma J, Goding Sauer A, Newman LA, Jemal A. Breast cancer statistics, 2017, racial disparity in mortality by state. *CA: Cancer J Clin* (2017) 67(6):439–48. doi: 10.3322/caac.21412
- Siegel RL, Miller KD, Fuchs HE, Jemal A. Cancer statistics, 2022. *CA: Cancer J Clin* (2022) 72(1):7–33. doi: 10.3322/caac.21708
- Chen W, Zheng R, Baade PD, Zhang S, Zeng H, Bray F, et al. Cancer statistics in China, 2015. *CA: Cancer J Clin* (2016) 66(2):115–32. doi: 10.3322/caac.21338

## Supplementary material

The Supplementary Material for this article can be found online at: <https://www.frontiersin.org/articles/10.3389/fimmu.2022.927565/full#supplementary-material>

### SUPPLEMENTARY FIGURE 1

Difference analysis of immune scores (A) and stromal scores (B) in normal/tumor, age (age over 40 years old was defined as the old group, age up to 40 years was defined as the young group), T stage, N stage, TNM stage. Statistical difference was compared by pairwise comparisons using Wilcoxon test. Significance: \* $P < 0.05$ ; \*\* $P < 0.01$ ; \*\*\* $P < 0.001$ ; ns, not significant. Kaplan-Meier analysis between low and high immune group (C)/stromal group (D) (low and high immune/stromal group was divided by the average value).

### SUPPLEMENTARY FIGURE 2

The PCA (A) and t-SNE (B) analysis between low and high TME-risk group. PCA, principal-component analysis; t-SNE, t-distributed stochastic neighbor embedding.

### SUPPLEMENTARY FIGURE 3

Kaplan-Meier analysis between low and high TME-risk group in stage I (A), stage II (B), stage III (C), HR positive breast cancer patients (D), Her-2 positive breast cancer patients (E) and TNBC patients (F). TME, tumor microenvironment; HR, hormone receptor; Her-2, human epidermal growth factor receptor 2; TNBC, triple negative breast cancer.

### SUPPLEMENTARY FIGURE 4

Kaplan-Meier analysis and Immunohistochemical staining of the TME-risk signature, including SLIT3 (A), TNN (B), IGHD (C), KLRB1 (D), and TCN1 (E). TME; tumor microenvironment.

### SUPPLEMENTARY FIGURE 5

The UMAP results of single cell sequencing of the TME-risk signature, including SLIT3 (A), TNN (B), IGHD (C), KLRB1 (D), and TCN1 (E). TME, tumor microenvironment.

### SUPPLEMENTARY FIGURE 6

GSEA analysis (including GO and KEGG analysis) between low and high TME-risk groups (top 50 listed biological function in BP (A), CC (B), MF (C) and KEGG (D), (FDR  $q$ -value  $< 0.05$  and  $|NES| > 1$ )). GSEA, gene set enrichment analysis; GO, gene ontology; KEGG, Kyoto Encyclopedia of Genes and Genomes.

### SUPPLEMENTARY FIGURE 7

Association between immune scores (A), stromal scores (B), tumor purity (C), and TME-risk scores and their distribution in the low and high TME-risk groups. Association between 5 screening genes (SLIT3 (D), TNN (E), IGHD (F), KLRB1 (G), TCN1 (H)) and TME-risk scores and their distribution in the low and high TME-risk groups. TME, tumor microenvironment.

- Xia C, Dong X, Li H, Cao M, Sun D, He S, et al. Cancer statistics in China and united states, 2022: profiles, trends, and determinants. *Chin Med J* (2022) 135(5):584–90. doi: 10.1097/cm9.0000000000002108
- Jamal-Hanjani M, Quezada SA, Larkin J, Swanton C. Translational implications of tumor heterogeneity. *Clin Cancer Res an Off J Am Assoc Cancer Res* (2015) 21(6):1258–66. doi: 10.1158/1078-0432.Ccr-14-1429
- Fayanju OM, Park KU, Lucci A. Molecular genomic testing for breast cancer: Utility for surgeons. *Ann Surg Oncol* (2018) 25(2):512–9. doi: 10.1245/s10434-017-6254-z

8. Buyse M, Loi S, van't Veer L, Viale G, Delorenzi M, Glas AM, et al. Validation and clinical utility of a 70-gene prognostic signature for women with node-negative breast cancer. *J Natl Cancer Institute* (2006) 98(17):1183–92. doi: 10.1093/jnci/djj329
9. Mook S, Schmidt MK, Viale G, Pruneri G, Eekhout I, Floore A, et al. The 70-gene prognosis-signature predicts disease outcome in breast cancer patients with 1–3 positive lymph nodes in an independent validation study. *Breast Cancer Res Treat* (2009) 116(2):295–302. doi: 10.1007/s10549-008-0130-2
10. van de Vijver MJ, He YD, van't Veer LJ, Dai H, Hart AA, Voskuil DW, et al. A gene-expression signature as a predictor of survival in breast cancer. *N Engl J Med* (2002) 347(25):1999–2009. doi: 10.1056/NEJMoa021967
11. van't Veer LJ, Dai H, van de Vijver MJ, He YD, Hart AA, Mao M, et al. Gene expression profiling predicts clinical outcome of breast cancer. *Nature* (2002) 415(6871):530–6. doi: 10.1038/415530a
12. Jiang YZ, Ma D, Suo C, Shi J, Xue M, Hu X, et al. Genomic and transcriptomic landscape of triple-negative breast cancers: Subtypes and treatment strategies. *Cancer Cell* (2019) 35(3):428–40 e5. doi: 10.1016/j.ccell.2019.02.001
13. Deepak KGK, Vempati R, Nagaraju GP, Dasari VR, Nagini S, Rao DN, et al. Tumor microenvironment: Challenges and opportunities in targeting metastasis of triple negative breast cancer. *Pharmacol Res* (2020) 153:104683. doi: 10.1016/j.phrs.2020.104683
14. Hanahan D, Coussens LM. Accessories to the crime: functions of cells recruited to the tumor microenvironment. *Cancer Cell* (2012) 21(3):309–22. doi: 10.1016/j.ccr.2012.02.022
15. Hanahan D, Weinberg RA. Hallmarks of cancer: the next generation. *Cell* (2011) 144(5):646–74. doi: 10.1016/j.cell.2011.02.013
16. Krug K, Jaehnig EJ, Satpathy S, Blumenberg L, Karpova A, Anurag M, et al. Proteogenomic landscape of breast cancer tumorigenesis and targeted therapy. *Cell* (2020) 183(5):1436–56.e31. doi: 10.1016/j.cell.2020.10.036
17. Wang S, Xiong Y, Zhang Q, Su D, Yu C, Cao Y, et al. Clinical significance and immunogenomic landscape analyses of the immune cell signature based prognostic model for patients with breast cancer. *Briefings Bioinf* (2021) 22(4). doi: 10.1093/bib/bbaa311
18. Bussard KM, Mutkus L, Stumpf K, Gomez-Manzano C, Marini FC. Tumor-associated stromal cells as key contributors to the tumor microenvironment. *Breast Cancer Res BCR* (2016) 18(1):84. doi: 10.1186/s13058-016-0740-2
19. Tajbakhsh A, Hasanazadeh M, Rezaee M, Khedri M, Khazaei M, ShahidSales S, et al. Therapeutic potential of novel formulated forms of curcumin in the treatment of breast cancer by the targeting of cellular and physiological dysregulated pathways. *J Cell Physiol* (2018) 233(3):2183–92. doi: 10.1002/jcp.25961
20. Velaei K, Samadi N, Barazvan B, Soleimani Rad J. Tumor microenvironment-mediated chemoresistance in breast cancer. *Breast (Edinburgh Scotland)* (2016) 30:92–100. doi: 10.1016/j.breast.2016.09.002
21. Nwabo Kamdje AH, Seke Etet PF, Vecchio L, Muller JM, Krampera M, Lukong KE. Signaling pathways in breast cancer: therapeutic targeting of the microenvironment. *Cell Signal* (2014) 26(12):2843–56. doi: 10.1016/j.cellsig.2014.07.034
22. Akbulut H, Babahan C, Abgarmi SA, Ocal M, Besler M. Recent advances in cancer stem cell targeted therapy. *Crit Rev Oncogenesis* (2019) 24(1):1–20. doi: 10.1615/CritRevOncog.2018029574
23. Zhu P, He F, Hou Y, Tu G, Li Q, Jin T, et al. A novel hypoxic long noncoding RNA KB-1980E6.3 maintains breast cancer stem cell stemness via interacting with IGF2BP1 to facilitate c-Myc mRNA stability. *Oncogene* (2021) 40(9):1609–27. doi: 10.1038/s41388-020-01638-9
24. Amornsupak K, Insawang T, Thuwajit P, OC P, Eccles SA, Thuwajit C. Cancer-associated fibroblasts induce high mobility group box 1 and contribute to resistance to doxorubicin in breast cancer cells. *BMC Cancer* (2014) 14:955. doi: 10.1186/1471-2407-14-955
25. Mueller KL, Madden JM, Zoratti GL, Kuperwasser C, List K, Boerner JL. Fibroblast-secreted hepatocyte growth factor mediates epidermal growth factor receptor tyrosine kinase inhibitor resistance in triple-negative breast cancers through paracrine activation of met. *Breast Cancer Res BCR* (2012) 14(4):R104. doi: 10.1186/bcr3224
26. Mehraj U, Ganai RA, Macha MA, Hamid A, Zargar MA, Bhat AA, et al. The tumor microenvironment as driver of stemness and therapeutic resistance in breast cancer: New challenges and therapeutic opportunities. *Cell Oncol (Dordr)* (2021) 44(6):1209–29. doi: 10.1007/s13402-021-00634-9
27. Olson OC, Kim H, Quail DF, Foley EA, Joyce JA. Tumor-associated macrophages suppress the cytotoxic activity of antimitotic agents. *Cell Rep* (2017) 19(1):101–13. doi: 10.1016/j.celrep.2017.03.038
28. Yoshihara K, Shahmoradgolgi M, Martu<sup>ll</sup>nez E, Vegesna R, Kim H, Torres-Garcia W, et al. Inferring tumour purity and stromal and immune cell admixture from expression data. *Nat Commun* (2013) 4:2612. doi: 10.1038/ncomms3612
29. Wu J, Li L, Zhang H, Zhao Y, Zhang H, Wu S, et al. A risk model developed based on tumor microenvironment predicts overall survival and associates with tumor immunity of patients with lung adenocarcinoma. *Oncogene* (2021) 40(26):4413–24. doi: 10.1038/s41388-021-01853-y
30. De Simone M, Arrighoni A, Rossetti G, Gruarin P, Ranzani V, Politano C, et al. Transcriptional landscape of human tissue lymphocytes unveils uniqueness of tumor-infiltrating T regulatory cells. *Immunity* (2016) 45(5):1135–47. doi: 10.1016/j.immuni.2016.10.021
31. Johnston RJ, Su LJ, Pinckney J, Critton D, Boyer E, Krishnakumar A, et al. VISTA is an acidic pH-selective ligand for PSGL-1. *Nature* (2019) 574(7779):565–70. doi: 10.1038/s41586-019-1674-5
32. Li B, Severson E, Pignon JC, Zhao H, Li T, Novak J, et al. Comprehensive analyses of tumor immunity: implications for cancer immunotherapy. *Genome Biol* (2016) 17(1):174. doi: 10.1186/s13059-016-1028-7
33. Newman AM, Liu CL, Green MR, Gentles AJ, Feng W, Xu Y, et al. Robust enumeration of cell subsets from tissue expression profiles. *Nat Methods* (2015) 12(5):453–7. doi: 10.1038/nmeth.3337
34. Aran D, Hu Z, Butte AJ. xCell: digitally portraying the tissue cellular heterogeneity landscape. *Genome Biol* (2017) 18(1):220. doi: 10.1186/s13059-017-1349-1
35. Charoentong P, Finotello F, Angelova M, Mayer C, Efremova M, Rieder D, et al. Pan-cancer immunogenomic analyses reveal genotype-immunophenotype relationships and predictors of response to checkpoint blockade. *Cell Rep* (2017) 18(1):248–62. doi: 10.1016/j.celrep.2016.12.019
36. Yu S, Wang Y, Peng K, Lyu M, Liu F, Liu T. Establishment of a prognostic signature of Stromal/Immune-related genes for gastric adenocarcinoma based on ESTIMATE algorithm. *Front Cell Dev Biol* (2021) 9:752023. doi: 10.3389/fcell.2021.752023
37. Wang H, Wu X, Chen Y. Stromal-immune score-based gene signature: A prognosis stratification tool in gastric cancer. *Front Oncol* (2019) 9:1212. doi: 10.3389/fonc.2019.01212
38. Jia J, Dai Y, Zhang Q, Tang P, Fu Q, Xiong G. Stromal score-based gene signature: A prognostic prediction model for colon cancer. *Front Genet* (2021) 12:655855. doi: 10.3389/fgene.2021.655855
39. Ma Q, Chen Y, Xiao F, Hao Y, Song Z, Zhang J, et al. A signature of estimate-stromal-immune score-based genes associated with the prognosis of lung adenocarcinoma. *Trans Lung Cancer Res* (2021) 10(3):1484–500. doi: 10.21037/tlcr-21-223
40. Xu WH, Xu Y, Wang J, Wan FN, Wang HK, Cao DL, et al. Prognostic value and immune infiltration of novel signatures in clear cell renal cell carcinoma microenvironment. *Aging* (2019) 11(17):6999–7020. doi: 10.18632/aging.102233
41. Dieci MV, Radosevic-Robin N, Fineberg S, van den Eynden G, Ternes N, Penault-Llorca F, et al. Update on tumor-infiltrating lymphocytes (TILs) in breast cancer, including recommendations to assess TILs in residual disease after neoadjuvant therapy and in carcinoma in situ: A report of the international immuno-oncology biomarker working group on breast cancer. *Semin Cancer Biol* (2018) 52(Pt 2):16–25. doi: 10.1016/j.semcancer.2017.10.003
42. Denkert C, von Minckwitz G, Darb-Esfahani S, Lederer B, Heppner BI, Weber KE, et al. Tumour-infiltrating lymphocytes and prognosis in different subtypes of breast cancer: a pooled analysis of 3771 patients treated with neoadjuvant therapy. *Lancet Oncol* (2018) 19(1):40–50. doi: 10.1016/s1470-2045(17)30904-x
43. Dhaouadi S, Murdamoothoo D, Tounsi A, Erne W, Benabderrazek R, Benlasfar Z, et al. Generation and characterization of dromedary tenascin-c and tenascin-W specific antibodies. *Biochem Biophys Res Commun* (2020) 530(2):471–8. doi: 10.1016/j.bbrc.2020.05.077
44. Degen M, Scherberich A, Tucker RP. Tenascin-W: Discovery, evolution, and future prospects. *Front Immunol* (2020) 11:623305. doi: 10.3389/fimmu.2020.623305
45. Dai CF, Jiang YZ, Li Y, Wang K, Liu PS, Patankar MS, et al. Expression and roles of Slit/Robo in human ovarian cancer. *Histochem Cell Biol* (2011) 135(5):475–85. doi: 10.1007/s00418-011-0806-2
46. Ng L, Chow AKM, Man JHW, Yau TCC, Wan TMH, Iyer DN, et al. Suppression of Slit3 induces tumor proliferation and chemoresistance in hepatocellular carcinoma through activation of GSK3 $\beta$ /H $\beta$ -catenin pathway. *BMC Cancer* (2018) 18(1):621. doi: 10.1186/s12885-018-4326-5
47. Guan H, Wei G, Wu J, Fang D, Liao Z, Xiao H, et al. Down-regulation of miR-218-2 and its host gene SLIT3 cooperate to promote invasion and progression of thyroid cancer. *J Clin Endocrinol Metab* (2013) 98(8):E1334–44. doi: 10.1210/jc.2013-1053
48. Kim M, Kim JH, Baek SJ, Kim SY, Kim YS. Specific expression and methylation of SLIT1, SLIT2, SLIT3, and miR-218 in gastric cancer subtypes. *Int J Oncol* (2016) 48(6):2497–507. doi: 10.3892/ijo.2016.3473
49. Zhu X, Yi K, Hou D, Huang H, Jiang X, Shi X, et al. Clinicopathological analysis and prognostic assessment of transcobalamin I (TCN1) in patients with colorectal tumors. *Med Sci Monit Int Med J Exp Clin Res* (2020) 26:e923828. doi: 10.12659/msm.923828

50. Lee YY, Wei YC, Tian YF, Sun DP, Sheu MJ, Yang CC, et al. Overexpression of transcobalamin 1 is an independent negative prognosticator in rectal cancers receiving concurrent chemoradiotherapy. *J Cancer* (2017) 8(8):1330–7. doi: 10.7150/jca.18274
51. Liu GJ, Wang YJ, Yue M, Zhao LM, Guo YD, Liu YP, et al. High expression of TCN1 is a negative prognostic biomarker and can predict neoadjuvant chemosensitivity of colon cancer. *Sci Rep* (2020) 10(1):11951. doi: 10.1038/s41598-020-68150-8
52. Kuri-Magaña H, Collado-Torres L, Jaffe AE, Valdovinos-Torres H, Ovilla-Muñoz M, Téllez-Sosa J, et al. Non-coding class switch recombination-related transcription in human normal and pathological immune responses. *Front Immunol* (2018) 9:2679. doi: 10.3389/fimmu.2018.02679
53. Gentles AJ, Newman AM, Liu CL, Bratman SV, Feng W, Kim D, et al. The prognostic landscape of genes and infiltrating immune cells across human cancers. *Nature Medicine* (2015) 21(8):938–45. doi: 10.1038/nm.3909
54. Abbott M, Ustoyev Y. Cancer and the immune system: The history and background of immunotherapy. *Semin Oncol Nursing* (2019) 35(5):150923. doi: 10.1016/j.soncn.2019.08.002
55. Yang Y. Cancer immunotherapy: harnessing the immune system to battle cancer. *J Clin Invest* (2015) 125(9):3335–7. doi: 10.1172/jci83871
56. van den Bulk J, Verdegaal EM, de Miranda NF. Cancer immunotherapy: broadening the scope of targetable tumours. *Open Biol* (2018) 8(6). doi: 10.1098/rsob.180037
57. Cimen Bozkus C, Roudko V, Finnigan JP, Mascarenhas J, Hoffman R, Iancu-Rubin C, et al. Immune checkpoint blockade enhances shared neoantigen-induced T-cell immunity directed against mutated calreticulin in myeloproliferative neoplasms. *Cancer Discov* (2019) 9(9):1192–207. doi: 10.1158/2159-8290.Cd-18-1356
58. Liu L, Bai X, Wang J, Tang XR, Wu DH, Du SS, et al. Combination of TMB and CNA stratifies prognostic and predictive responses to immunotherapy across metastatic cancer. *Clin Cancer Res an Off J Am Assoc Cancer Res* (2019) 25(24):7413–23. doi: 10.1158/1078-0432.Ccr-19-0558
59. Hellmann MD, Ciuleanu TE, Pluzanski A, Lee JS, Otterson GA, Audigier-Valette C, et al. Nivolumab plus ipilimumab in lung cancer with a high tumor mutational burden. *N Engl J Med* (2018) 378(22):2093–104. doi: 10.1056/NEJMoa1801946
60. Song Y, Zeng S, Zheng G, Chen D, Li P, Yang M, et al. FOXO3a-driven miRNA signatures suppresses VEGF-A/NRP1 signaling and breast cancer metastasis. *Oncogene* (2021) 40(4):777–90. doi: 10.1038/s41388-020-01562-y
61. Zhang L, Chen Y, Wang H, Zheng X, Li C, Han Z. miR-376a inhibits breast cancer cell progression by targeting neuropilin-1 NR. *OncoTargets Ther* (2018) 11:5293–302. doi: 10.2147/ott.S173416
62. Li K, Ma L, Sun Y, Li X, Ren H, Tang SC, et al. The immunotherapy candidate TNFSF4 may help the induction of a promising immunological response in breast carcinomas. *Sci Rep* (2021) 11(1):18587. doi: 10.1038/s41598-021-98131-4